ALMA Memo #319
Photonic Local Oscillators for Radio Astronomy: Signal-to-Noise Issues

Bill Shillue

National Radio Astronomy Observatory

Tucson, AZ

August 9, 2000

1   Abstract

An investigation is made into the signal-to-noise requirements of a photonic local oscillator (LO). Simple theoretical expressions are given for the RF power, relative-intensity-noise (RIN), shot noise and zero-point noise, and measurements are made that verify the simple theory. The theory is then used to determine what photomixer current and noise levels will be required for ALMA receivers, and to predict how much wideband noise will be added to the receiver by the photonic LO. For ALMA, implementation of the photonic LO includes the transmission of two wavelengths of light by optical fiber over distances as great as 25 km. There is an optical fiber nonlinearity called stimulated Brillouin scattering (SBS), which limits the amount of light that can be transmitted by fiber over long distances. As a result, in some cases, an optical amplifier may be required at the antenna end of the fiber.

2   Introduction

It has been estimated that coherent millimeter/submillimeter sources can be developed by laser photomixing for generation of up to 100 microwatts of power as high as 3 THz [1]. This has been proposed as a means of providing the local oscillator for ALMA receivers. Within the ALMA project, this has been called the *direct photonic* local oscillator scheme, in which photomixing of two lasers separated by a given radio difference frequency results in a widely tunable local oscillator. The photonic LO was investigated in an earlier ALMA memo in order to prove the viability of the approach [2]. This memo discusses more details of the approach, and presents measurements that have been made of the LO power and noise characteristics.

It should be pointed out that the current baseline plan for ALMA is to use a photonic scheme only to supply a reference to which millimeter-wave oscillators at each telescope are phase locked. The local oscillator would be supplied by a sequence of electronically tunable YIG oscillators, amplifiers, and multipliers [3]. The photomixer RF power required for the photonic reference scheme is much less than for the direct photonic LO. In fact, it has been demonstrated that commercially available photomixer devices are already available that have sufficient RF power [4]. Also, the wideband noise is not an important issue for the photonic reference scheme, because in that case photomixer noise is only present close to the carrier due to the limited bandwidth of the phase-lock-loop. Noise from the oscillator-multiplier chain is present, however, and the contribution from those components is treated in [5]. The discussion that follows pertains mainly to the direct photonic local oscillator scheme.

From a set of very basic considerations, this memo will show that:

- Photomixer generated RF power and associated noise can be accurately estimated from simple expressions.

- It is best to pump the photomixer with as much light as possible in order to maximize signal-to-noise ratio. This will reduce the noise added to the receiver and increase the LO power available to the SIS mixer.

- Lasers should be chosen that have relaxation resonance noise peaks outside of the ALMA IF band of 4-12 GHz.

- In some cases stimulated Brillouin scattering will limit the amount of light transmitted via fiber over long distances.

- The Relative-Intensity-Noise (RIN) of the lasers should be minimized. This implies the use of very high-power, low-RIN lasers and minimizing the number of optical amplifiers.

With regard to all of the considerations of signal-to-noise requirements and LO transmission by optical fiber treated in this memo, all indications are that in theory the direct photonic LO will work. The only real obstacle is the development of adequate photomixers to 300 GHz and higher frequencies.

3   RF Power

In the general case, two lasers of different power level incident upon a photomixer will develop an RF output power of:

$$P_{rf} = \frac{1}{2}I_{rf}^2 R_L(1 - |\Gamma|^2), \tag{1}$$

where I_{rf} is the peak-to-peak RF current developed across the load, R_L is the load resistance, and Γ is the reflection coefficient of the diode relative to the load. In most commercial photomixers, the photomixer acts like a true current source with a current proportional to the optical input power:

$$I_{dc} = rP_{opt}, \tag{2}$$

where r is the responsivity calculated from the quantum efficiency, η, of the photomixer by Eq. A1. A typical photodiode model includes a parallel resistance and capacitance in parallel with the current source. In many commercial photomixers, the photodiode is connected directly to a 50-ohm transmission line and output connector. Thus the mismatch between the photodiode and the load, Γ, can be quite large. In appendix A, a simple model is presented for the case of two lasers of unequal power incident upon a photomixer. Then using Eq. A8, we can rewrite Eq. 1 as

$$P_{rf} = 2I_{dc1}I_{dc2}R_L(1 - |\Gamma|^2), \tag{3}$$

where I_{dc1} and I_{dc2} are the DC currents in the photomixer due to each of the two lasers. Eq. 3 also implies that for a given amount of total optical power, the RF power is maximized when the optical power is equally split between the two laser sources.

As a simple example, if we assume equal contributions of 0.5 mW from each lasers, then $A_1 = A_2$ and for $R_L = 50$ ohms, $\eta = 0.5$, and $\lambda = 1550$ nm, (and assuming $\Gamma = 0$)[Note: these parameters will be use for examples throughout Sec. 3, 4, and 6], we get :

$$I_{dc} = 0.626\,mA \qquad P_{rf} = 9.8\,\mu W. \tag{4}$$

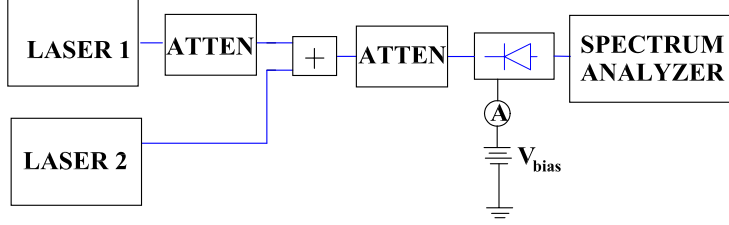Notice that the RF power increases as the square of the optical power.

Figure 1: Setup for Measuring RF Power versus photodiode current

3.1   Measurement of RF Power

A simple experiment confirms the expressions for RF power. Fig. 1 shows an experimental setup in which two lasers are combined together and input to a photomixer. The lasers are then tuned to a 2.0 GHz beatnote, well within the photomixer bandwidth, and then input to a spectrum analyzer. The laser amplitudes are made equal by adjustment of the first attenuator. The second attenuator is then used to vary the optical power incident upon the photomixer. Fig. 2 shows the RF power vs. DC photocurrent for both the theoretical and measured cases. Notice that the RF power increases as the square of the optical input and photodetector current as expected. A constant refelction coefficient of $|\Gamma| = 0.79$ was used to account for mismatch and any resistive losses, and after applying that factor the theoretical and experimental curves are in good agreement.

4   Noise

4.1   Shot Noise

The quantization of DC current results in shot noise given by:

$$i_{rms}^2 = 2eI_{dc}\Delta f, \tag{5}$$

which is the rms current fluctuation in bandwidth Δf, and

$$P_{\text{shot}} = i_{rms}^2 R_L = 2eI_{dc}\Delta f R_L, \tag{6}$$

which is the noise power delivered to the load. T_{shot} is the equivalent noise temperature, defined in the usual way as:

$$T_{shot} = \frac{P_{\text{shot}}}{k\Delta f} = \frac{2e}{k}I_{dc}R_L. \tag{7}$$

Using the same parameter values as before ($P_{opt1} = 0.5$ mW, $P_{opt2} = 0.5$ mW, $r = 0.626$ A/W, and $R_L = 50$ ohms) gives $P_{\text{shot}} = $ -170 dBm/Hz which is equivalent to $T_{\text{shot}} = 726°K$. Note from Eq. 8 that the shot noise is proportional to the photodetector current.

4.2   Zero-Point Noise

There is zero-point fluctuation noise associated with each of the optical carriers. Unlike in the microwave regime, zero-point noise is much higher than thermal noise at optical frequencies [6]. Zero-point fluctuation noise is generated in the photomixer by beating between the laser signals and
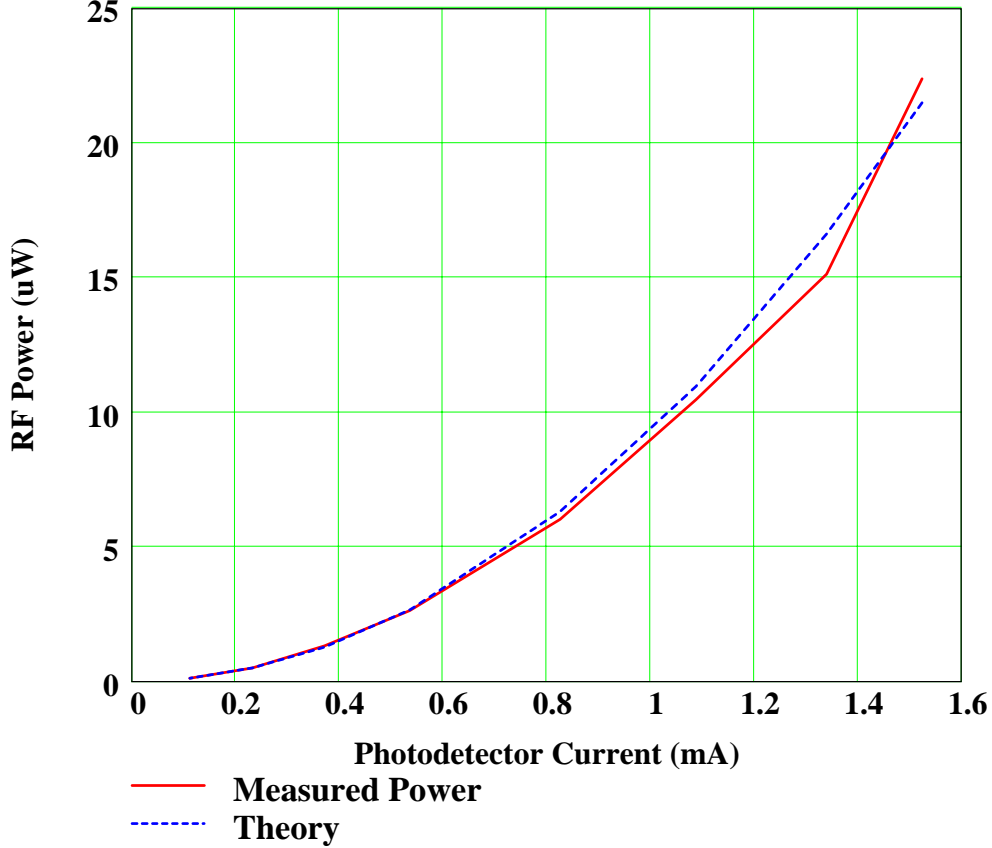
Figure 2: RF Power(mW) vs DC Photocurrent(mA) for heterodyne of two lasers having equal intensity. Beatnote frequency is 2.0 GHz. (An RF coupling of $1 - |\Gamma^2| = 0.37$ was used to match the theoretical curve to the measured result)

the zero-point noise, $h\nu/2$, associated with the optical frequency. The zero-point noise temperature is given by [2]:

$$T_{zp} = \frac{2\eta e}{k} I_{dc} R_L. \tag{8}$$

It is seen to differ from the shot noise only by the factor η, so that in our example case ($\eta = 0.5$), $T_{zp} = 363° K$.

4.3 Thermal Noise

There is also thermal noise at the physical temperature of the photomixer, but this may be negligible if the photomixer is cooled. The thermal noise is dependent on the photodetector current only to the extent that it gives rise to a change in the device temperature.

4.4 Laser Relative Intensity Noise

Laser RIN is usually given in units of dBc/Hz, and denotes the ratio of mean squared fluctuation current per unit bandwidth to the squared DC current after detection. The expressions for noise
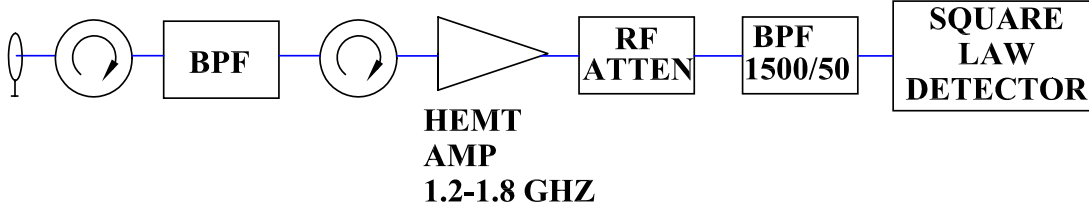
4

Figure 3: Low noise receiver setup for measurement of photomixing noise

power and temperature due to RIN are [2]:

$$P_{rin} = i_{rms}^2 R_L \Delta f = I_{dc}^2 N_{ri} R_L \Delta f \tag{9}$$

$$T_{rin} = \frac{I_{dc}^2 N_{ri} R_L}{k}. \tag{10}$$

If we take a reasonable RIN value of $N_{ri} = -155$ dBc/Hz, in our example this gives $P_{rin} = -172$ dBm/Hz or $T_{rin} = 448°K$. Note that the RIN noise is proportional to the photodetector current squared. It may happen that the RIN level is different for each of the two lasers. In this case, the DC current level contributed by each laser is used to calculate an rms noise current from each laser. These are then square summed to get the total noise current and noise power.

4.5   Measurement of Noise from Photomixing

The noise from a photomixer was measured using a 1.5 GHz low-noise receiver, as shown in Fig. 3. The receiver amplifier is preceded by two isolator stages to eliminate reflections between the photomixer and the HEMT amplifier. Filters are used before and after the amplifier and the measurement bandwidth is 50 MHz. A high-speed (20 GHz) commercial photomixer was used, and the coaxial output was connected directly to the low-noise receiver. It was generally found that there were noise components proportional to the photomixer current (shot and zero-point noise) and to the current squared (RIN noise), and a constant noise component (thermal), as predicted by the theory. The noise temperature of the receiver was measured using a hot and cold 50-ohm coaxial load.

By using the photomixer in detector mode, with a single laser input, the different noise components can be determined. This was done for a 1550-nm fixed-wavelength fiber laser with a 40 mW output power level (suitably attenuated), and for a widely-tunable external cavity diode laser. The total noise temperature was measured and broken down into a shot and zero-point noise component and a RIN noise component and plotted as a function of the photodetector current, which is directly proportional to the input optical power. This is done in Fig. 4 for the fiber laser. The shot and zero-point component is derived by solving for the noise that varies linearly with the photodetector current. This results in $T_{\text{shot}} + T_{zp}$=789 deg K/mA. The measured values for the photomixer used in the experiment were $r = 0.84$ and $\eta = 0.67$. The theoretical result is then $T_{\text{shot}} + T_{zp}$=1937 deg K/mA. This is reconciled by a coupling loss of $1 - |\Gamma^2|$=0.40 which is very close to the value measured for the RF power. Thus, the shot noise and zero-point noise components, like the RF signal power, are well behaved and very well described by the theory.
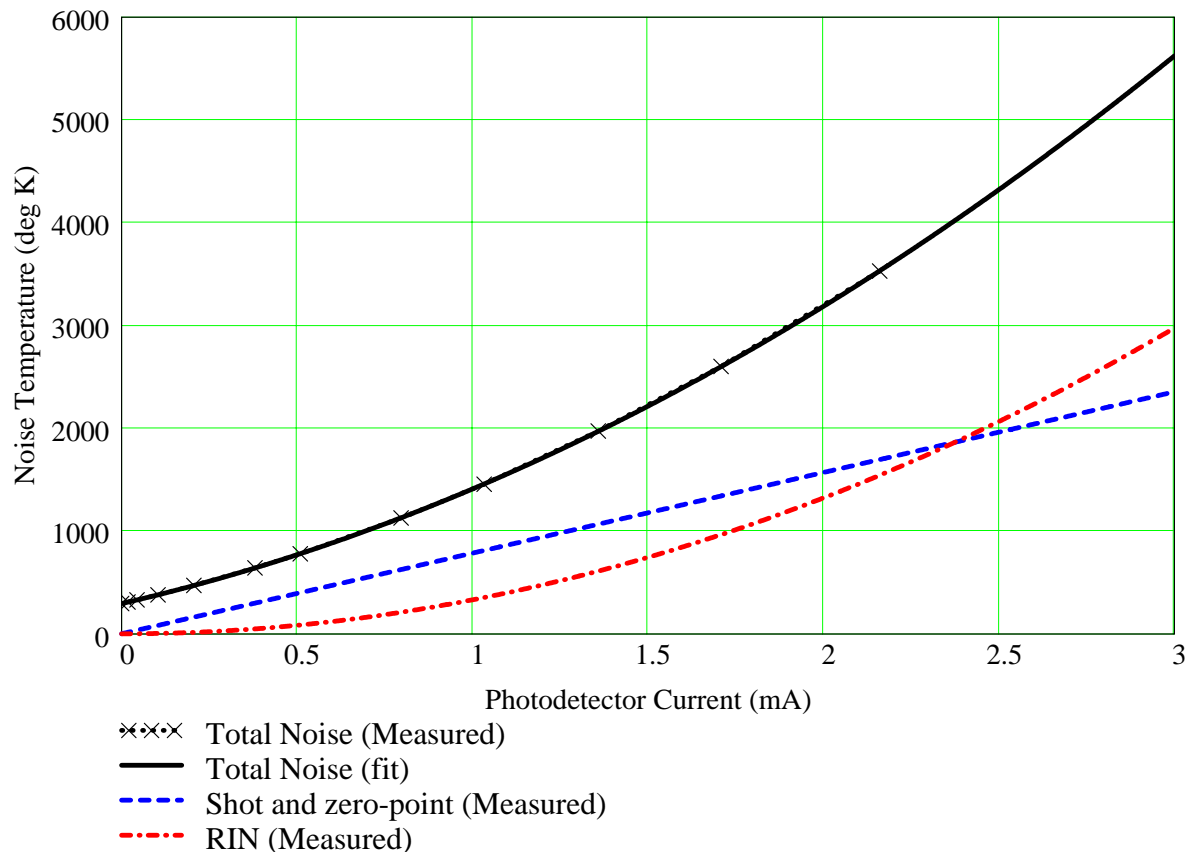
5

Figure 4: Noise Temperature (deg K) vs Photocurrent(mA). A power coupling ratio of 0.40 from source to load was used to match the shot and zero point noise, and this resulted in a derived RIN noise level of -159 dBc/Hz

Having extracted the linear noise terms, we can subtract off the fixed thermal noise (300 deg K), and be left with the RIN noise which varies quadratically with the photodetector current. In this way, we calculate the RIN of the fiber laser to be -159 dBc/Hz. The measurement was repeated for the diode laser, yielding similar results but a slightly higher RIN of -156.6 dBc/Hz at peak rated output power.

5   Relaxation resonance in diode lasers

RIN is not a well specified quantity by most laser manufacturers. Sometimes it is specified as being below some value, like -150 dBc/Hz, which is the limit of the manufacturer's measurement ability. Others do not specify it at all. If possible, it is a good idea to find out how it has been measured, and at what frequency, offset, and bandwidth.

There is another noise component from the laser that must not be overlooked. This is the relaxation resonance that results in noise peaking at a fixed offset frequency from the laser. The physical effect that causes the resonance is the same mechanism that limits the modulation frequency in diode lasers, a relation between the time constants of stimulated emission and photon lifetime in the laser. For most diode lasers this noise peaking occurs in the 500 MHz to 10 GHz range. The relaxation resonance occurs at a frequency given by [7]:

$$\omega_r^2 = \frac{G_n \times (I - I_{th})}{q}. \tag{11}$$

where G_n is a complex physical parameter describing the change in laser gain per unit length versus change in carrier population density. I is the laser current and I_{th} is the threshold current. In general, then, the resonant frequency depends on the laser current, temperature, geometry, and material parameters of the laser diode.

Our main concern is that the relaxation resonance could add to the receiver noise temperature if it appears in the 4-12 GHz ALMA IF bandwidth. Any laser considered for use on ALMA will have to be measured to check the noise vs. offset frequency. The G_n term in Eq. 11 is inversely dependent on the laser cavity volume, so the smaller the laser diode, the higher the relaxation resonance frequency. The fiber laser used in our experiments has a cavity that is about 20 meters long, and the relaxation resonance occurs at about 70 kHz, so it will not contribute additional wideband noise in the ALMA IF bandwidth. (The phase noise added at 70 kHz is negligible).

To investigate the wideband noise properties of the diode laser, both lasers were used to illuminate the photomixer, and the heterodyne beatnote frequency was varied from 1.8 GHz to 13.5 GHz. The lasers were not phase locked, but the relative stability was on the order of 10 MHz on the time scale of the measurement. Since we were using a 1.5 GHz receiver, this means that we were measuring the noise at offsets of from 300 MHz to 12.0 GHz from the beatnote. The result of this measurement is shown in the lower curve of Fig. 5.

The plot shows several peaks and a fairly flat noise level in the absence of the peaks. The flat level, most evident from 4-12 GHz, is the noise due to the laser RIN, and the constant contributions from the other noise terms. The strong resonant peak at about 2.8 GHz and secondary peak at 3.7 GHz are due to the relaxation resonances of the laser diode. Below 1 GHz, the noise level begins to increase due to the near-in noise on the laser.

5.1   Noise Added by Fiber Amplifier

A fiber amplifier was inserted between the lasers and the photomixer, followed by an optical attenuator which was adjusted so that the photomixer current was the same as it was before. The fiber amplifier has ASE (amplified spontaneous emission) noise which appears in the beatnote by mixing with the optical signals or by ASE noise mixing with ASE noise. These noise processes are characterized by a noise figure which has a minimum value of 3 dB for a high gain fiber amplifier [18]. Optical amplifiers are different from RF amplifiers in fundamental ways, and much effort has been devoted recently to the definition of a noise figure that would be suitable for both RF and optical amplifiers [19, 20].

Here we make the assumption that the dominant source of noise at the input of the optical amplifier will be from laser RIN. In fact, RIN is defined as a signal-to-noise ratio, so the signal-to-noise ratio after the optical amplifier should degrade by the noise figure of the amplifier. In our experiment we used an optical amplifier with a noise figure of 5 dB. Using the previously derived RIN levels for the two lasers, we would expect to measure $T_{rin} = 380°K$ without the optical amplifier. With the optical amplifier, this RIN contribution should increase by 5 dB, to $1200°K$. Therefore, an additional noise temperature of $820°K$ is expected. The upper curve of Fig. 5 shows the measured value of the noise temperature with the optical amplifier in place, and the additional noise measured was actually $1000°K$, a number which is relatively independent of frequency offset. This is reasonably close to what is expected.

A rigorous analysis would have to be undertaken to account for all of the noise sources in this configuration of an optical amplifier and attenuator placed between the laser sources and the detector. The measurement presented here is meant mainly to show that there is a finite amount of noise added by the optical amplifier, and that to first order it is predictable.
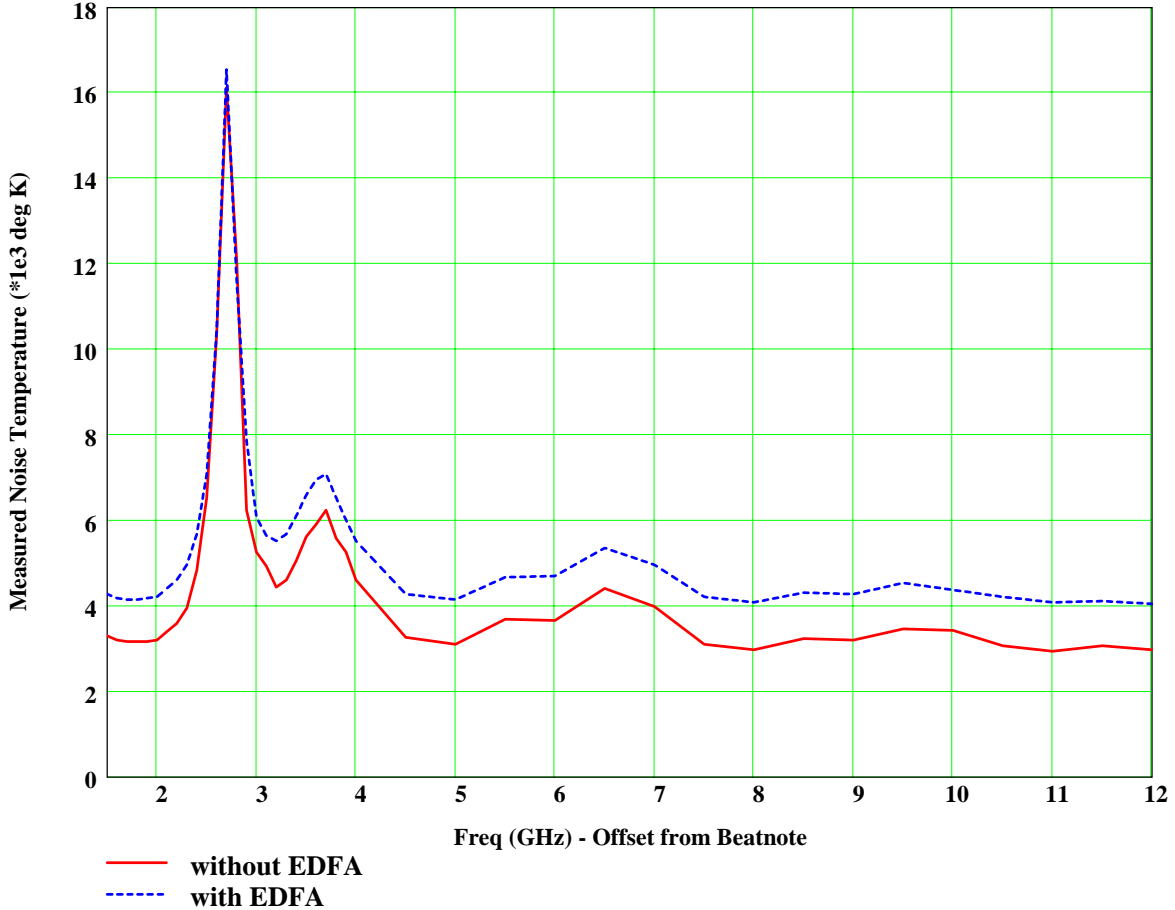
Figure 5: Measured Noise temperature versus frequency as a function of the frequency offset from the beatnote. The receiver was tuned to 1.5 GHz and the beatnote was tuned from 3.0–13.5 GHz. Addition of an optical amplifier increases the noise level but does not change the resonance. $I_{dc1}=I_{dc2}=0.620$ mA for both cases.

6   LO Noise Added to Receiver

In the examples from sections 3,4 and 6, the photodetector was illuminated by 0.5mW from each laser. The calculated RF output power is $9.8\,\mu W$ for a perfectly matched load. Then there are contributions of 1090 K from shot and zero-point noise, 446 K from RIN noise, and a small amount of thermal noise. The amount of LO power required to be available to the receiver input, and the amount required to actually pump the SIS mixer will both depend on a number of factors such as: receiver frequency, number of junctions in the SIS mixer, mixer configuration, and LO coupling scheme [8]. Suppose that $10\,\mu W$ is required at the mixer flange, and $1\,\mu W$ is actually incident on the SIS device. Our example case would have (roughly) the required LO power at the receiver flange, and a noise contribution of $(1090 + 446 + 300)/10 = 184°K/\mu W$ will also be seen by the mixer. For a single-ended mixer, this is clearly a significant and unacceptable amount of added noise.

There are two possible remedies for this. The first is that some bands will have balanced mixers which will provide some rejection of the LO noise (See ALMA memo #308 [9]). The second is that as long as shot noise is the dominant contributor to the overall LO noise, S/N improvement will result from an increase in the photomixer power level. If more light is available to the photomixer,
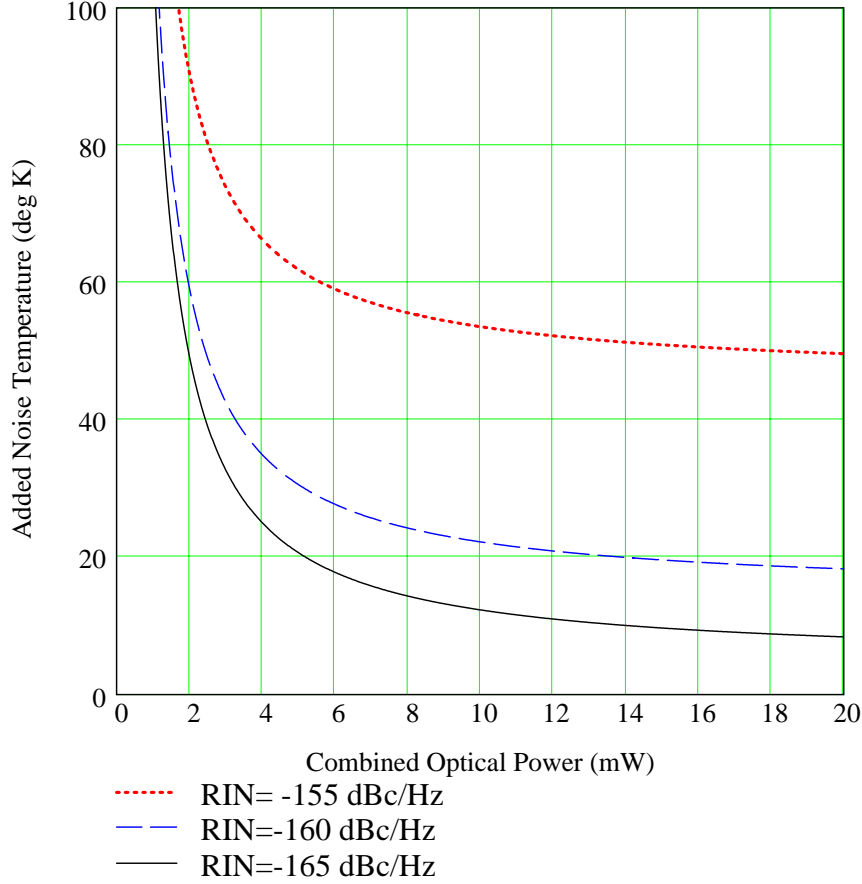
Figure 6: Total noise per microwatt of RF power as a function of the amount of light input to the photomixer. Equal power is incident from each laser. Parameter is Laser RIN level. No rejection of LO noise from balanced mixer or LO diplexer is included.

then RF output power will increase as the square of the light power, and shot noise will increase only linearly. Eventually, RIN induced noise, which is also quadratic with light power, will exceed shot noise, and no further S/N gain will be possible.

The result of this is shown in Figure 6. The plot shows the total noise contribution from the photonic local oscillator normalized to one microwatt of RF power, as a function of the combined optical power input. If the optical power is increased to more than several milliwatts, then the signal-to-noise, expressed in the plot as added noise temperature per microwatt of RF power, is increased to a level limited ultimately by the laser RIN. Three RIN levels are plotted: -155 dBc/Hz, -160 dBc/Hz, and -165 dBc/Hz. If we want to limit the noise added by the LO to less than $20°K$, then a RIN of -155 dBc/Hz will be too high. For the case of a balanced mixer, or a Martin-Puplett which is configured to give some LO noise rejection, the added noise is expected to be reduced by 10 dB or more.

6.1 Implications for ALMA

The signal-to-noise measurements presented here have significant implications for the ALMA systems design if a direct photonic LO is implemented. To get the best signal-to-noise, the ideal situation will be to increase the light input into the photomixer until RIN noise is the biggest noise term. Any further increase of the light into the device will yield little improvement in signal-to-noise.

There will also be a need for stabilization of the LO power to the receiver for ALMA. This could be done quite easily by attenuation of the optical input into the photomixer. However, the discussion above implies that the lowest noise occurs with the maximum amount of light input (assuming the photomixer does not saturate). Thus, leveling the LO with an optical attenuator will result in the maximum amount of noise for a given LO power into the mixer, which is undesirable. Leveling of the photonic local oscillator via active control of the photomixer bias may be possible but has not been tested. Generally, the photomixer bias is operated at a level such that all of the depletion layer carriers are at saturation velocity. By operating the bias just below this level, active control of the bias may achieve the desired control of the RF power. A study of this effect would have to answer the questions of whether the bias adjustment decreases the signal-to-noise, and whether the bias adjustment affects the phase of the LO. Also, bias control may work on one type of photomixer but not on another, as the junction design, materials, doping levels, and the bias circuits of some of the leading candidate photomixers are quite different [10, 11, 12].

This discussion assumes that there is a "given" laser and photomixer, but the devices deserve some discussion themselves. The photomixer current can only be increased until saturation or self-heating limits the output power. It may also be true in some cases that increasing the current level in the device causes a reduction in the device speed due to carrier screening effects. In fact, many of the best published results on high-speed, wide bandwidth photomixers are based upon pulsed rather than CW-measurements [10, 13]. However, the effect of saturation and thermal heating is quite different for a pulsed device, and therefore the CW heterodyne measurement is essential to the evaluation of photomixer devices as photonic local oscillators for radio astronomy. As for the lasers, there are several critical parameters: linewidth, tuning resolution and repeatability, output power, sidemode suppression, ...etc. However, assuming that the laser can be phase-locked so that the wavelength jitter and near-in phase noise are adequate, the parameter that is most important for signal-to-noise ratio is the laser RIN. RIN can be caused by many different types of physical phenomena, but very low RIN lasers are usually limited by spontaneous emission in the laser. Since the level of spontaneous emission is not strongly dependent on the laser pump level, the lasers with the best RIN specification are likely to be very high power lasers. Thus it may be preferable to use a high power laser source rather than a low power laser and an optical amplifier, because the optical amplifier will increase the overall RIN level, contributing its own spontaneous emission.

As an example of the dependence of RIN on laser pump level, for the New Focus ECDL laser used in these measurements, the RIN level for a diode current of 57 mA and output power of 3.7 mW was -153 dBc/Hz, but this was reduced to -159.4 dBc/Hz at 98 mA and 9.1 mW output power.

7 Fiber Nonlinearity

Stimulated Brillouin Scattering (SBS) is an effect whereby light that is input to a fiber is reflected back because of a moving index variation in the fiber. This is caused by acoustic vibrations induced at high input power levels [14]. The effect results in a power-distance relationship that limits the amount of power that can be transmitted by a narrow linewidth source on fiber over a given distance. The SBS scattering mechanism results in light that is reflected back towards the source but not forward. Also, the reflected light undergoes a frequency downshift of between 10-11 GHz, depending on the material characteristics of the fiber. This is fortunate for round-trip correction, because the frequency
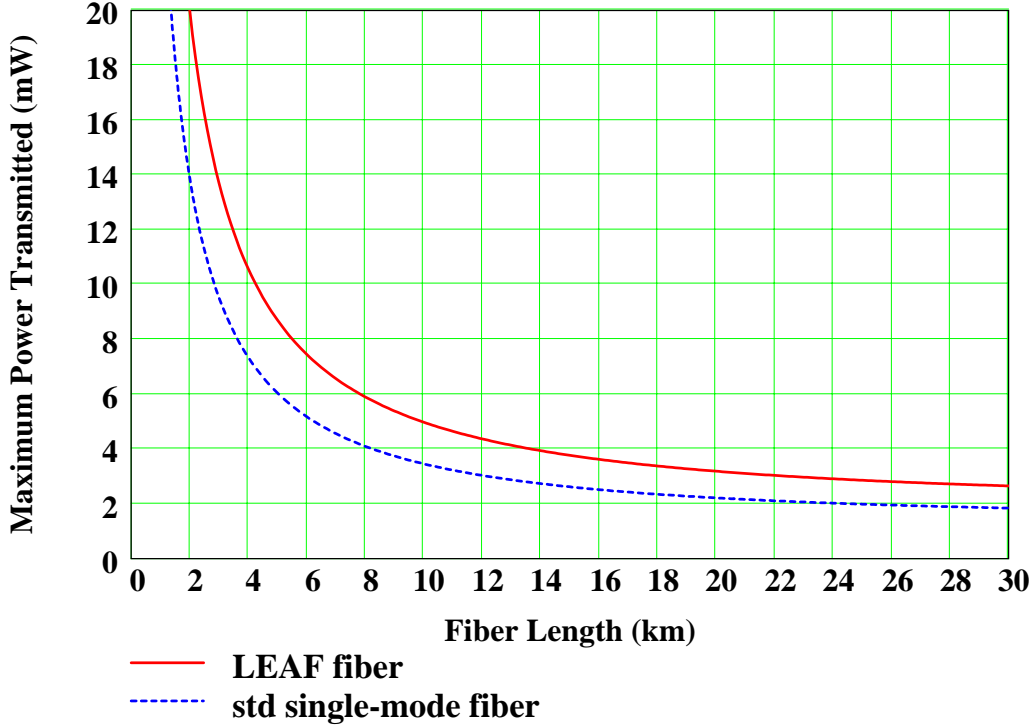
Figure 7: Maximum transmitted power for narrow linewidth sources for two types of 1550 nm single mode fiber. Power is limited by Stimulated Brillouin Scattering.

shift isolates the desired return signal and the undesired Brillouin scattered light. A critical power is defined at which the scattered power is equal to the power launched from the end of the fiber [14]:

$$P_{\text{crit}} = \frac{21 \times A_{eff}}{g_b L_{eff}} \tag{12}$$

where A_{eff} is the effective area of the fiber and L_{eff} is the effective length of the fiber defined as follows:

$$L_{eff} = \frac{1 - e^{-\alpha l}}{\alpha}, \tag{13}$$

where α is the fiber attenuation coefficient (m^{-1}), roughly $4.6 \times 10^{-5}\, m^{-1}$ for 0.2 dB/km fiber. The effective length is less than the actual length because of fiber attenuation. The Brillouin gain coefficient, g_b, is 4×10^{-9} cm/W. The greater the effective area or the shorter the fiber, the more light that you can get into the fiber before the onset of Brillouin scattering. The telecommunications industry has used Corning SMF-28 or its equivalent for years as the standard single-mode fiber at 1550 nm, which has a cross-sectional area of about $50\,\mu\text{m}^2$. However, more recently, partly to mitigate the effect of SBS for long fiber links, Corning LEAF (large effective area fiber) has been introduced with a larger effective area of $72\,\mu\text{m}^2$. As an example, for a LEAF fiber of length 25 km
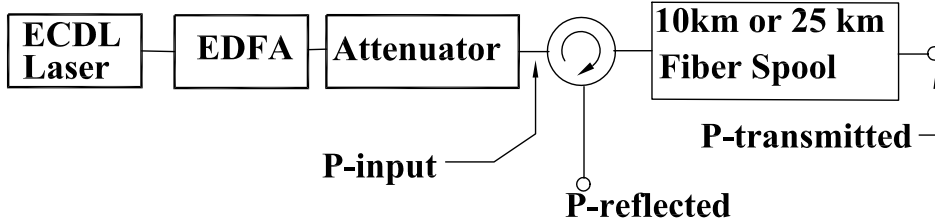
11

Figure 8: Setup for test of Stimulated Brillouin Scattering (SBS).

at 1550 nm, and effective length of 14.85 km, the critical power is 2.5 mW over a distance of 25 km. The critical power for both the LEAF fiber and standard 1550-nm single mode fiber is plotted in Fig. 7. The LEAF fiber gives a 44 percent increase in the power-distance factor. This fiber is being manufactured for large quantities at cost as low as the SMF-28 fiber.

An SBS test was performed in which 50 mW of light at a single wavelength was input to LEAF optical fiber. Two lengths of fiber were used, 10 km and 25 km. The setup is shown in Fig. 8. The transmitted and reflected power were measured as a function of the input power level. Results very close to those predicted in Fig. 7 were measured. The measurement results are plotted in Fig. 9. A maximum power of 8.6 mW (higher than predicted) and 2.3 mW (lower than predicted) was measured for 10 km and 25 km, respectively. No change in the scattering behavior was noticed as the polarization of the light going into the fiber was changed (using a fiber polarization rotator). The plot shows the transmitted and reflected power level for 10 km and 25 km spools, and also the transmitted power that would occur if the fiber was linear with just 0.2 dB/km insertion loss. It is clear from looking at the plot that the maximum useful input power level is limited to about 15 mW and 10 mW for 10 km and 25 km, respectively.

The effect of SBS is mitigated for light sources which have a linewidth of more than about 20 MHz, which is the Brillouin gain bandwidth [15]. However, this is not expected to be the case for ALMA, especially if a very narrow linewidth master laser is used for round-trip correction [16]. A very important implication is that the limit applies to the individual lasers rather than the combined laser power. More simply, the output limit at 25 km will be 4.6 mW, or 2.3 mW for each laser.

Modulating, or dithering, of one or both laser sources is a technique that has been proven to overcome the effects of SBS [17]. For the ALMA project, the addition of an optical fiber amplifier at each antenna, or perhaps only at the antennas at great distance from the central station, should easily overcome power limitation imposed by SBS. The drawbacks include some additional system complexity, a modest cost increase, and possibly increased LO noise.

7.1   ALMA Case Study

An ALMA case study is presented here as an example of what might be required for a direct photonic implementation. Since the question of how much power is required for pumping the SIS mixer depends on a number of things such as the receiving frequency, number of SIS junctions, and the configuration of the mixer, an enormous simplification is made here by assuming that ten microwatts of available LO power will be sufficient. It is further assumed that there is a balanced mixer arrangement with 10 dB of LO noise suppression. A factor of two power loss due to mismatch and insertion loss is assumed in the photomixer output circuit. A worst case distribution length of 25 km is assumed.
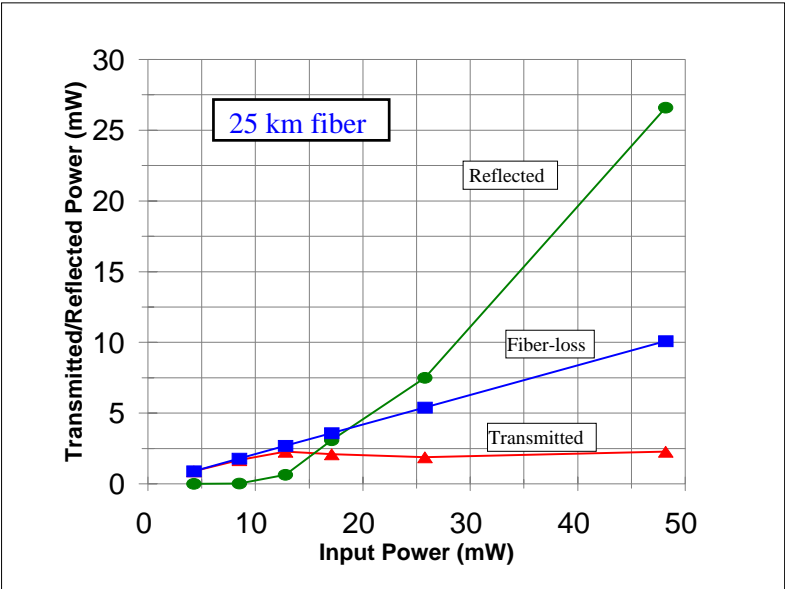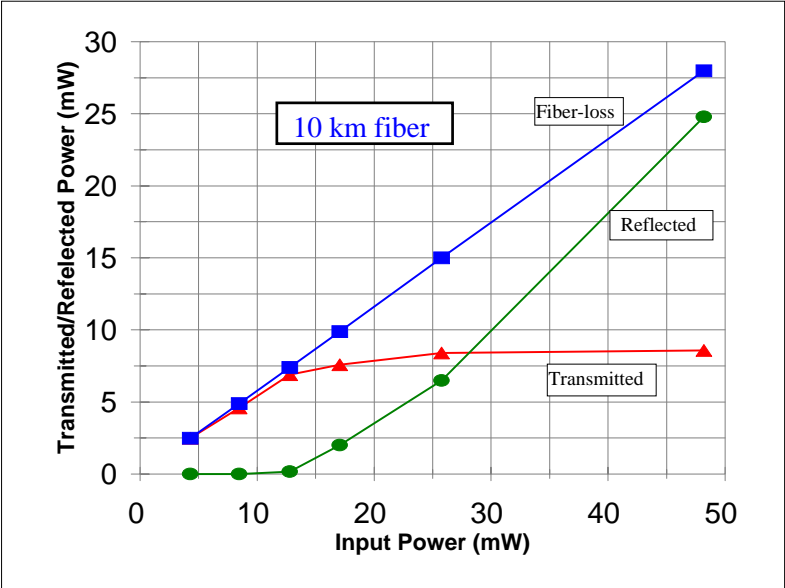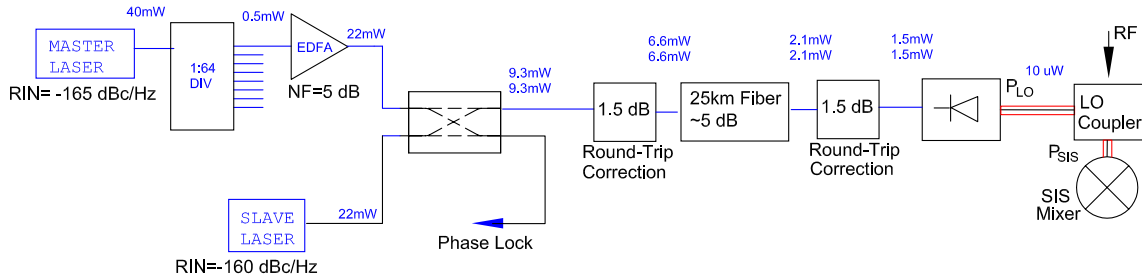
12

Figure 9: Test of the effect of Stimulated Brillouin Scattering on the Transmitted and Reflected Power Levels through 10 km and 25 km lengths of Corning Large-Effective Area Fiber. Also shown (Fiber-loss) is the expected transmission level just from the standard fiber loss of 0.2 db/km.

Figure 10: ALMA Direct Photonic Case Study

Fig. 10 is a sketch of a strawman power distribution scheme for a direct photonic LO. Ten microwatts (after 3 dB RF loss) is developed by the photomixer by an RF current of 0.90 mA (0.64 mA rms current). Assuming a responsivity of 0.3 mA/mW for the photomixer, an optical input level of 3.0 mW is required from the two sources right at the input to the photomixer. Since this is split equally between the two sources, there is no appreciable Brillouin scattering. A small loss of 1.5 dB is estimated for each end of the fiber to account for coupling and connector losses in the round-trip correction. An input optical power of 6.6 mW at each wavelength is required at the source end of the 25 km fiber. This translates back to 22 mW required from each laser source before the optical combiner. If the master laser is common to all antennas, then a distribution network consisting of splitters and optical amplifiers will be required. The requirement of 22 mW from the slave laser may be difficult to find in an inexpensive commercial unit, in which case an optical amplifier may be required there as well.

There are two distinct regimes of operation which will be determined by the characteristics of the SIS device, receiver characteristics, and photomixer performance:

1. Relatively low power required into the photomixer, shot noise dominated, and a balanced mixer arrangement for LO noise rejection.

2. Higher LO power required for noise reduction, RIN and SBS-scattering are the dominant effects, and an optical amplifier at the antenna end is required for the longer baselines.

The example shown here is of the first type. The total noise is dominated by shot noise. With

10 dB isolation, there is 133 deg K total noise input to the mixer, or 15.8 deg K per microwatt of RF power.

We could just as easily have chosen to highlight the second type. If the isolation were not available, for example if the SIS mixer were single ended, then the photomixer would have to be driven to higher level to reduce the overall noise. For instance, the input to the photomixer would be about 10 mW of optical power, and the LO power out of the photomixer would be on the order of 100 microwatts. In this case, an optical amplifier would be required at the antenna end for the longest baselines to overcome SBS.

8   Conclusion

Many considerations for the implementation of a photonic local oscillator for radio astronomy millimeter/submillimeter receivers have been given. This memo did not discuss the design and development of photomixers with sufficient output power in the frequency range of 100 GHz–1 THz, which is still a big technological hurdle. However, many other topics which will be important for a photonic local oscillator were discussed. This includes simple theoretical expressions for the RF power, shot noise, and RIN-noise resulting from the photomixer conversion. Also, effects like the relaxation resonance of diode lasers and Stimulated Brillouin Scattering in the fiber transmission were discussed. It was recommended that lasers of lowest possible RIN be selected and tested. Also, for the most distant antennas in the array (more than 10 km from the central building), it may be necessary to have a fiber amplifier at the antenna to circumvent the effect of Brillouin scattering.

9   Acknowledgements

References

[1] U. Gliese, "THz Source Based On Laser Mixing," International Topical Meeting on Microwave Photonics. MWP '97, Sep. 3-5, 1997, pp. 87-90

[2] J.M. Payne, L.D. D'Addario, D.T. Emerson, A.R. Kerr, B. Shillue, "Photonic Local Oscillator for the Millimeter Array," SPIE Conference on Advanced Technology for MMW, Radio, and Terahertz Telescopes, Kona, Hawaii, March, 1998, SPIE Vol. 3357, pp. 143-151, Also ALMA memo #200, http://www.alma.nrao.edu/memos

[3] R.F. Bradley, "Wide Bandwidth, YIG-Based Sources and Modern Frequency Multipliers for the MMA Local Oscillator Sytem," ALMA memo #207, April 1998, http://www.alma.nrao.edu/memos

[4] B. Shillue, "Millimeter-wave RF Power Measurements of a Commercial Photomixer," ALMA Memo #313, June 2000, http://www.alma.nrao.edu/memos

[5] E. Bryerton, D.L. Thacker, K. Saini, R. Bradley, "Noise Measurements of YIG-Tuned Oscillator Sources for the ALMA LO," ALMA memo #311, pending, http://www.alma.nrao.edu/memos

[6] A. R. Kerr, M. J. Feldman, S.-K. Pan, "Receiver Noise Temperature, the Quantum Noise Limit, and the Role of the Zero-Point Fluctuations," MMA Memo #161, September 10, 1996

[7] G.P. Agrawal, N.K. Dutta, *Long-Wavelength Semiconductor Lasers*, Van Nostrand Reinhold Co., New York, 1986, p. 246

[8] Belitsky, V., "Local Oscillator Power Requirements for ALMA SIS Mixers", ALMA Memo #264, May, 1999, http://www.alma.nrao.edu/memos

[9] A. R. Kerr, S.-K. Pan, A. W. Lichtenberger, N. Horner, J. E. Effland, and K. Crady, "A Single-Chip Balanced SIS Mixer For 200-300 GHz", ALMA Memo #308, May, 2000, http://www.alma.nrao.edu/memos

[10] N. Shimizu, N. Watanabe, T. Furuta, and T. Ishibashi, "InP-InGaAs Uni-Traveling Carrier Photodiode With Improved 3-dB Bandwidth of Over 150 GHz," IEEE Photonics Technology Letters, Vol. 10, No. 3, March 1998, pp. 412-414

[11] G. Unterborsch, A. Umbach, D. Trommer, G.G. Mekonnen, "70 GHz Long Wavelength Photodetector," Proc. of the 23rd European Conference on Optical Communications, ECOC '97, Edinburgh, UK, Sept. 22-25, 1997, pp. 25-28.

[12] A. Stohr, R. Heinzelmann, C. Kaczmarek, D. Jager, "Ultra-broadband Ka- to W-band 1.55 m travelling-wave photomixer," Electronics Letters, vol. 36, no. 11, 25th May, 2000, p. 970-972

[13] L.Y. Lin, M.C. Wu, T. Itoh, T.A. Vang, R.E. Muller, D.L. Sivco, and A.Y. Cho, "Velocity-Matched Distributed Photodetectors with High-Saturation Power and Large Bandwidth," IEEE Photonics Technology Letters, Vol. 8., No. 10, Oct. 1996, pp. 1376-1378.

[14] Pollock, C., *Fundamentals of Optoelectronics*, Richard D. Irwin, Inc., 1995, pp. 199-200

[15] Andrew R. Chraplyvy, "Limitations on Lightwave Communications Imposed by Optical-Fiber Nonlinearities," Invited Paper, IEEE Journal of Lightwave Technology, Vol. 8, No. 10, October, 1990, pp. 1548-1557.

[16] J. Payne, B. Shillue, A. Vaccari, "Photonic Techniques for Use on the Atacama Large Millimeter Array," ALMA Memo #267, June, 1999, http://www.alma.nrao.edu/memos

[17] F.W. Willems, M. Wuys, J.S. Leong, "Simultaneous Suppression of Stimulated Brillouin Scattering and Interferometric Noise in Externally Modulated Lightwave AM-SCM Systems," IEEE Photonics Technology Letters, Vol. 6, No. 12, Dec. 1994, pp. 1476-1478.

[18] E. Desurvire, *Erbium-Doped Fiber Amplifiers*, Wiley and Sons, Inc., 1994, p. 100.

[19] A.R. Kerr, "Suggestions for Revised Definitions of Noise Quantities, including Quantum Effects" IEEE Transactions on Microwave Theory and Techniques, March 1999, Vol. 47, pp. 325-329.

[20] H. Haus, "Noise Figure Definition valid from RF to Optical Frequencies", IEEE Journal on Selected Topics in Quantum Electronics, March/April 2000, Vol. 6, pp. 240-247.

A   Appendix

A simple model for the case of two lasers of unequal power incident upon a photomixer is detailed.[1] Assume we have a photodetector of responsivity, r:

$$r = \eta e / h\nu = \eta e \lambda / hc \tag{A1}$$

where $\eta < 1$ is the quantum efficiency. We get $r =0.626$ A/W at $\lambda =1550$ nm and $\eta=0.5$; this is a realistic number. Let the optical input signal (from the two lasers) be represented by

$$A_{opt}(t) = A_1 \sin \omega_1 t + A_2 \sin \omega_2 t, \tag{A2}$$

The measurable quantity of the lasers is the time-averaged optical power, which we can write for the each individual laser:

$$P_{opt1} = \frac{A_1^2}{2} \qquad P_{opt2} = \frac{A_2^2}{2} \tag{A3}$$

and for the two lasers combined:

$$P_{opt} = P_{opt1} + P_{opt2} = \frac{A_1^2 + A_2^2}{2} \tag{A4}$$

and in terms of the DC photodetector current:

$$I_{dc} = I_{dc1} + I_{dc2} = \frac{rA_1^2}{2} + \frac{rA_2^2}{2} \tag{A5}$$

The lasers produce an average absorbed power in the photomixer of

$$P_{abs} = \frac{A_1^2}{2}\langle 1 - \cos^2 2\omega_1 t\rangle + \frac{A_2^2}{2}\langle 1 - \cos^2 2\omega_2 t\rangle + A_1 A_2 \langle \sin(\omega_1 - \omega_2)t - \sin(\omega_1 + \omega_2)t\rangle$$
$$= \frac{A_1^2 + A_2^2}{2} + A_1 A_2 \sin \omega_{rf} t$$

where $\omega_{rf} = \omega_1 - \omega_2$, and the last expression drops terms at optical frequencies and higher, on the grounds that the charge carrier mobility and external circuitry do not permit responses that fast. The output current is then:

$$I_{out} = rP_{abs} = r\left(\frac{A_1^2 + A_2^2}{2}\right) + rA_1 A_2 \sin \omega_{rf} t = I_{dc} + I_{rf}. \tag{A6}$$

This gives the relationship between the DC current and the RF current assuming that the photomixer bias and device physics do not otherwise limit the frequency response at ω_1. The RF output power can be expressed in terms of the RF current:

$$P_{rf} = \frac{1}{2}I_{rf}^2 R_L. \tag{A7}$$

Then substitution of Eq. A6 into Eq. A7 yields a very simple expression for the RF output power:

$$P_{rf} = 2I_{dc1}I_{dc2}R_L. \tag{A8}$$

Here I_{dc1} and I_{dc2} are the DC currents due to each of the lasers.

---

[1]This is extrapolated from the case of equal power lasers which was originally detailed by L. D'Addario in a private memo